

1. Alexandru IONEL

## PERFORMANCE EVALUATION OF PROPULSION SYSTEMS AS LEO DEORBITING DEVICES

1. INCAS – National Institute for Aerospace Research “Elie Carafoli”, Bucharest, ROMANIA

**Abstract:** This paper evaluates the possibility of deorbiting a launch vehicle upper-stage at end-of-mission from low Earth orbit, by using an additional propulsion system as the means of achieving deorbiting and complying to the ‘25 years’ mitigation regulation. The deorbiting performances of chemical and electrical propulsion are analyzed through a MATLAB code which integrates orbital perturbations such as gravitational acceleration, atmospheric drag and rocket engine/motor thrust. Additionally, the research is placed within a body of similar papers concerned with deorbiting by means of propulsion, by performing a state of the art study.

**Keywords:** deorbit, chemical propulsion, electric propulsion, MATLAB simulation, Hohmann transfer

### 1. MITIGATING ORBITAL DEBRIS

The Kessler Syndrome: in 1978, NASA scientists Burton Cour Palais and Donald Kessler determined that LEO debris would eventually have its leading source from spent rocket bodies and satellite collisions. Their predicted that debris from collisions would cause more collisions and debris, expanding exponentially the risk of active satellites in certain orbital regions. This chain reaction was coined collisional cascading by Kessler in a 1991 paper. February 2009 marked the prediction of the first catastrophic collision between the Russian Cosmos 2251 satellite and the Iridium 33 satellite, event which produced approximately 2200 trackable fragments, had a collision probability of one in 500,000 and a predicted miss distance of 584 m. Also, 3400 trackable fragments were produced by the 2007 Chinese antisatellite test. Cosmos 1934 collided in 1991 with the debris from the Russian Cosmos 1275 navigation and communication satellite. This collision took place in spite of a collision probability of one in 50,000, and a predicted miss distance of 512 m. Cerise, an active French reconnaissance satellite, collided in 1996 with debris from the launch of an Ariane 1 rocket, although the collision probability was one in 2,000,000 and the predicted miss distance was 882 m.

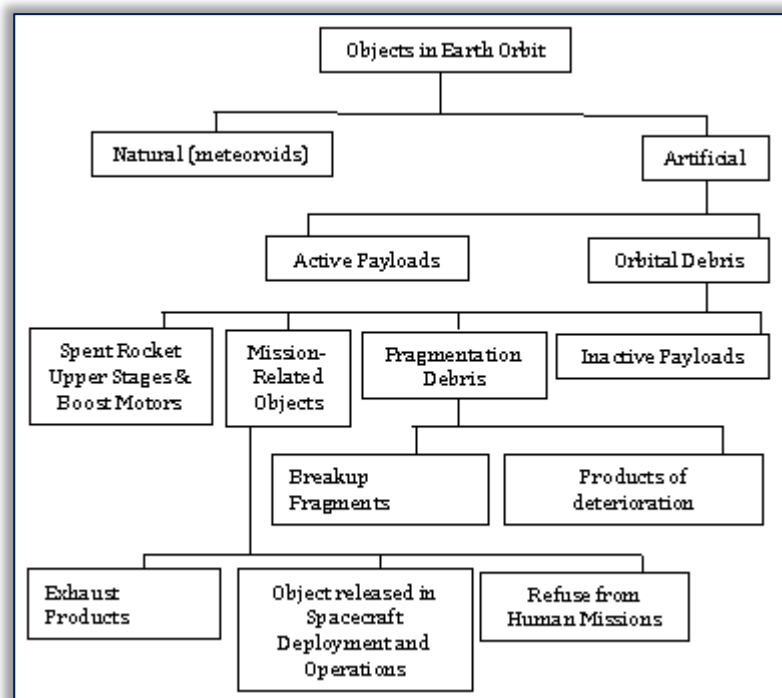


Figure 1. Classification of objects in Earth orbits [4]

Remediation and mitigation are significant problems besides establishing cause, number and risk of space debris. Remediation is concerned with cleaning the space environment through the removal of





debris. Mitigation is represented by the methods and policies which will lower the expansion rate of debris populations in the short term, and have been used for over 20 years. Mitigation methods include reducing or eliminating the discharge of space mission related debris, end-of-life passivation (eliminating energy sources – propellants, batteries, pressurants), and postmission disposal (reentering or moving an obsolete orbital object to a disposal orbit, or lowering its orbit so that it will reenter within 25 years) [1].

In Figures 1-3, classifications of objects in Earth orbit are given, taken from [4].

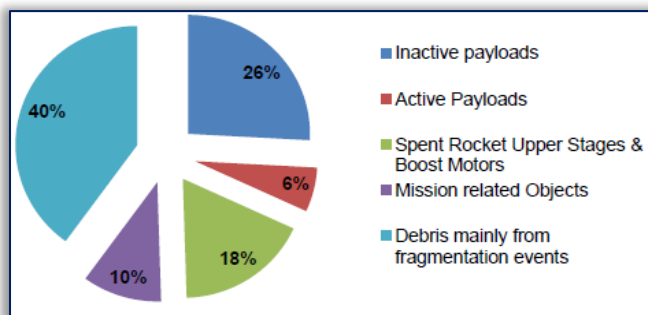


Figure 2. All catalogued space objects, classified by object type as of January 2002 [4]

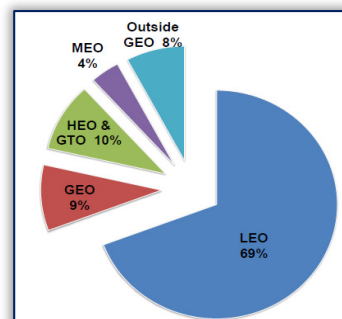


Figure 3. All catalogued space objects, classified by orbital region, as of January 2002 [4]

Inactive satellites and upper-stages are the main potential source of debris propagation, because of their large cross section that makes them statistically the most likely objects to be involved in a collision. In case of collision, their mass is so high that thousands of new debris can be generated, covering a broad spectrum of sizes [4].

## 2. PROPULSION SYSTEMS AS DEORBITING DEVICES

Controlled reentry is a Postmission Disposal (PMD) method of imposing a trajectory on an object, which causes it to reenter Earth's atmosphere, impacting in a certain area. This procedure eliminates the object from orbit, limiting hazards on ground, but requires an important quantity of propellant to achieve the orbit change required for reentry. Controlled reentry is best for launch vehicle upper stages as they have short mission time frames and can use the remaining mission propellant to accomplish the necessary orbital maneuvers [2]. According to [5], a de-orbit system should have specific characteristics:

- ☐ Reliability: the expectancy of the system not to function shall be lower than just leaving the spent satellite in orbit;
- ☐ Independence / autonomous: even if the satellite fails, the system must have power for its operation and be able to have simple communications with the satellite operating center;
- ☐ Applicability: the system must be capable of being applied to any satellite, not just a specific one;
- ☐ Storability: the subsystems must be capable of remaining fully operable for 15 years;
- ☐ Performance: the propellant mass for de-orbiting must be small in comparison to the satellite mass at the end of the mission.

[3] describes the possibilities of using additional propulsion subsystems, Table 1, to achieve deorbitation. Chemical propulsion systems have high thrust and low specific impulse (200 to 300 seconds), and therefore their most fuel efficient way of maneuvering to an orbit with a limited post-mission lifetime is to perform a small number of short-arc burns close to the apogee of the final mission orbit. Due to the high thrust levels over short time intervals, chemical propulsion is applicable to lowering the perigees for highly eccentric as well circular orbits. Electric propulsion systems usually have a low thrust and very high specific impulse (2000 to 4000 seconds), and therefore they perform a long duration, low thrust burn opposite to the velocity vector. This causes

Table 1. Propulsion systems [3]

	Advantages	Disadvantages
Solid Propulsion	<ul style="list-style-type: none"> <li>» Simple</li> <li>» Reliable</li> <li>» Low cost</li> <li>» High density</li> <li>» Low structural index</li> </ul>	<ul style="list-style-type: none"> <li>» One thrust per burn</li> <li>» Total impulse fix</li> <li>» Currently not qualified for long-term space applications</li> </ul>
Electrical Propulsion	<ul style="list-style-type: none"> <li>» Very high Isp</li> </ul>	<ul style="list-style-type: none"> <li>» Low thrust</li> <li>» Complex</li> <li>» Large maneuver time</li> <li>» Power consumption</li> </ul>
Bi-Propellant Propulsion	<ul style="list-style-type: none"> <li>» Wide thrust range</li> <li>» Modifiable</li> <li>» Proven</li> </ul>	<ul style="list-style-type: none"> <li>» Complex</li> <li>» Costly</li> <li>» Heavy</li> <li>» Toxic</li> </ul>

and therefore they perform a long duration, low thrust burn opposite to the velocity vector. This causes





a near-circular orbit to slowly spiral inwards, gradually reducing the altitude, until a sufficient atmospheric drag level is reached. Figures 1-3 from [3] indicate the specific impulse and thrust range of different propulsion systems. It is noted that the thrust varies over 10 orders of magnitude, while specific impulse varies over 2 orders of magnitude.

[4] makes a comparative study of deorbiting solutions, such as natural decay, drag augmentation devices, chemical propulsion, electrical propulsion and electrodynamic tether systems. For inclinations higher than 70 degrees, EP is the best option. CP is the worst solution regarding additional mass. For altitude lower than 500 km: CP is the most convenient option, ensuring the lowest deorbit time and ATP; EP is a viable option too, but it is more expensive than CP. For altitudes between 500 km and 700 km, chemical propulsion is the most viable option, along with EP, requiring lower total mass than CP, but with higher deorbit times and higher ATP. For the ranges between 700 km and 1500 km, CP and EP are the most optimal. For altitudes higher than 1500 km, both EP and CP are outperformed by EDT systems, Table 2.

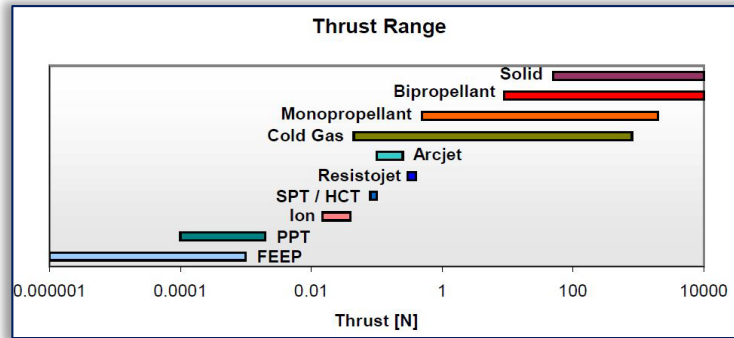


Figure 1. Thrust range of different propulsion systems [3]

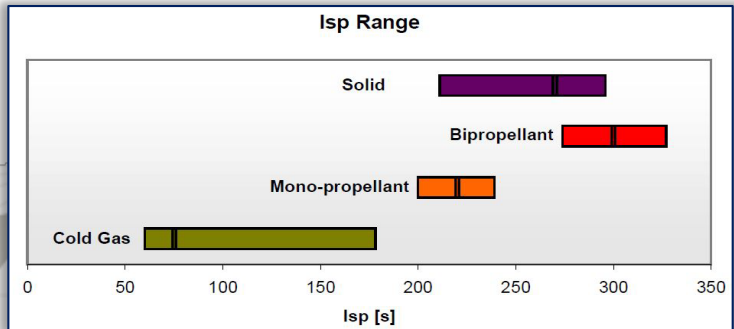


Figure 2. Specific impulse range of chemical propulsion systems [3]

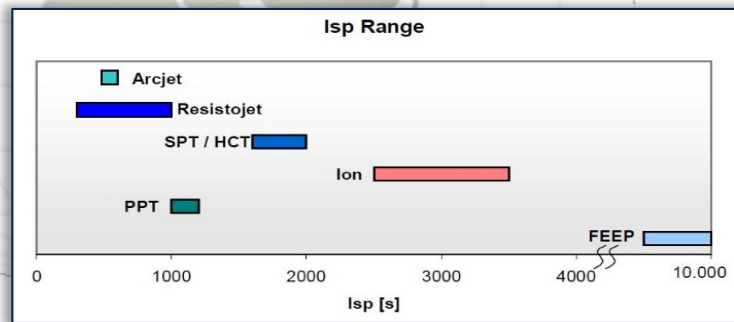


Figure 3. Specific impulse range of electrical propulsion systems [3]

Table 2. Numerical results of deorbit time and ATP (left), and additional mass (right) [4]

Initial Altitude [km]	Inclination [deg.]	Deorbit time Electrical Propulsion [years]	ATP Electrical Propulsion [sq. m x years]	Additional Mass Electrical Propulsion	Additional Mass Chemical Propulsion
800	65	0.44	1.18	67.23	99.94
900	65	0.5	1.34	70.97	115.5
1400	65	0.79	2.1	88.72	196.81
800	75	0.44	1.18	67.23	99.94
900	75	0.5	1.34	70.97	115.5
1400	75	0.79	2.1	88.72	196.81
800	82.5	0.44	1.18	67.23	99.94
900	82.5	0.5	1.34	70.97	115.5
1400	82.5	0.79	2.1	88.72	196.81
800	97.5	0.44	1.18	67.23	99.94
900	97.5	0.5	1.34	70.97	115.5
1400	97.5	0.79	2.1	88.72	196.81

According to [5], the strategy is to decrease the apogee velocity by use of solid propulsion systems, such that an orbit results with its perigee at 80 km altitude. Atmospheric drag then will rapidly decelerate and heat the satellite. Most satellite will burn up in the atmosphere. The required  $\Delta V$ 's in relation to altitude of the circular orbit are given in Table 2 from [5].





Table 3. Velocity increments for de-orbiting from various orbits to 80 km altitude [5]

De-orbit from: [km]	$\Delta V$ to 80 km [m/s]
500	121
1000	249
1500	362
2000	462
10000	1224
20000	1450

The de-orbit system is autonomous if it can rely on its own power source and electronics. Therefore the system needs to be equipped with small batteries; the capability to cut power to reaction wheels; means to determine the spacecraft's altitude; means to communicate with the Earth; means to operate the de-orbit electronics and to ignite the motors. For LEO spacecraft, data concerning the attitude may come from several GPS antennas mounted on the spacecraft.

[6] analyzes de-orbit strategies with low-thrusts provided by an electric propulsive system. The ELECTRA software was used, developed by CNES, which allows to assess the risks of doing victims on ground in case of launches or spacecraft re-entries failures, but also during and uncontrolled re-entry either for a long term re-entry of several years. The main objective of the paper consists of finding a way of decreasing dramatically the altitude of the satellites at the end of their lifetime in order to allow a re-entry within some hours without needing a large amount of propellant or a modification of the Attitude and Orbital Control Systems (AOCS), aspects which are prohibitive for small satellites. Study cases: the interest of semi-

controlled re-entries with low-thrust addresses mainly for small LEO satellites, because their size does not allow them to carry enough propellant to perform controlled re-entries. Thus, this strategy will be studied for three different satellites which are on a Sun-Synchronous Orbit, namely PARASOL, SMOS and SPOT-5. There exist different technologies of electric propulsion, such as Arcjet, Pulsed Plasma Thruster (SPT), Field Emission Electric Propulsion (FEEP), Ionic and Stationary Plasma Thruster (SPT). Thrust and specific impulse can be estimated for the imaginary electric propulsive system of the studied satellites. These values are given in Table 6 from [6].

According to [7], SPADES is a solid propulsion deorbiting system developed to support the compliance of future missions with the space debris mitigation requirements, Table 7, and can be used on: larger LEO satellites, upper stages and jettisoned components (e.g. SYLDA, SPELTRA), small satellites in LEO without propulsion system, multiple active debris removal missions.

### 3. RESEARCH METHODOLOGY

This paper will compare the performance of different propulsion system when deorbiting a 418 kg upper-stage at its end-of-mission. The propulsion systems that are analyzed are chemical and electrical, as shown in Table 8.

A cluster of motors that are fired as well sequentially as parallel, has a lower overall mass than one single dedicated de-orbit motor. An additional advantage is that a cluster of smaller motors can easier be implemented and integrated in the design than one single large motor. As numerical values, conclusions from the numerical simulations in [5], Table 4 gives some typical values for de-orbiting to 80 km. for each of the two  $\Delta V$  maneuvers 5.6 kg of solid propellant is required.

Table 4. Typical values for End Of Life satellite de-orbiting to 80 km [5]

Name	Unit	Satellite to 80 km at 0.004 g
Orbit altitude	[km]	780
Satellite mass (BOL)	[kg]	689
Satellite mass (EOL)	[kg]	574
Propellant mass	[kg]	115
Liquid propellant	-	Hydrazine
Solid propellant	-	AP-HTPB O/F=9.3, $\epsilon \sim 400$
Specific impulse	[s]	294
Density	[kg/m <sup>3</sup> ]	1825
Velocity increment	[m/s]	194.3
Required solid propellant	[kg]	44.9
Burn time with solid propellant	[s]	479

Table 5. Mass estimate of an autonomous de-orbit system

Part	Mass [kg]	Nr.	Total mass [kg]
Cluster of de-orbit motors (9/3)	6.57	9	59.13
Spin-up thruster	0.58	2	1.16
De-orbit electronics	1.5	1	1.5
Total mass of de-orbit system			62

Table 6. Imaginary propulsive characteristic for the studied satellites [6]

Satellite	Power [W]	Thruster	Thrust [mN]	Specific Impulse [s]
PARASOL	150	SPT	8	1500
SMOS	560	SPT	30	1500
SPOT-5	2400	SPT	150	1500
SPOT-5-like	2400	SPT	150	1500





Table 7. SPADES System Overview [7]

SPADES LEO 800km SSO - fully independent			
Mass	Host	dry	1336 kg
		wet (excluding adapter)	1429 kg
	SPADES	dry	139 kg
		wet	246 kg
Propulsion	Solid propellant system		
	4/2 cluster (4 SRMs, 2 firing simultaneously)		
	Providing de-orbit $\Delta V$ of 216 m/s with a $< 0.04$ g		
Power	Automatically activated in case of host power bus failure		
	Battery	Li-SOCl <sub>2</sub> primary battery	
		48 cells (826p) (1 redundant string)	
		Total energy: 643 Wh	
Bus	15 V regulated bus		
Communications	All S-Band system		
	2 x Transceiver		
	2 x fixed LGA for $2\pi$ coverage		
Thermal	MLI, heaters, black paint, SSM, radiator, heat switch		
	Internal (inside host) configuration for improved thermal conditions		
DHS	OBC	OSCAR based	
Structure	Support rings, adapter and support plates, brackets, interface rings		

Table 8. Propulsion systems studied in the numerical simulations

Propulsion Category		Engine	Thrust [N]	Isp [s]	Mass [kg]	Nr of used engines	
Chemical propulsion	Solid propulsion	Double base propellant	STAR 4G	306.927	269.4	1.49	4
		Bipropellant	R-4D	445	312	3.76	2
	Liquid propulsion	Monopropellant	MR-107	275	236	0.88	3
		Cold gas propellant	Sterer	12	68	0.174	6
Electric propulsion	Electro-thermal	Resistojet	MR-501B	0.3	300	0.89	4
		Arcjet	Primex MR-510	0.235	580	1.58	4
	Electro-static	Ion contact thruster	XIPS	0.015	2800	6.5	2
		Hall Effect Thruster	Fakel SPT-70	0.04	1510	1	2
	Electro-magnetic	PPT	Les 8/9	0.0003	600	5	2

An advantage of chemical propulsion is the preexistence of such a system on every spacecraft, i.e. the thruster used for the last orbit injection burn or thrusters used for attitude control, so the additional mass for deorbit would be only the additional propellant. A negative aspect of deorbiting with CP is the possible impact with meteoroids or debris of the propellant tanks in the necessary long operation life, although the risk of collision during deorbit is extremely low, due to the lowest ATP among all the different deorbit solutions. The best performing CP system would be the Liquid Oxygen/Liquid Hydrogen systems (LOX/LH), which have the problem of storing propellants at cryogenic temperatures. A second option is the Hypergolic Bi-propellant system, with Hydrazine (N<sub>2</sub>H<sub>4</sub>) and Dinitrogen Tetroxide (N<sub>2</sub>O<sub>4</sub>). The bipropellant system provides better performance than the monopropellant, but would imply an increased complexity of the hardware and higher inert mass, making the choice very expensive. The Hydrazine rocket engine requires the highest propellant mass fraction. Solid propulsion system is another considerable option, but it has a much lower reliability for deorbit application after years of onboard storage. The electric propulsion category is generally made of communications satellites whose antennas must be constantly pointed towards a specific ground station: hence, they need a continuous attitude control during their operational life. This implies that LEO satellites generally do not have an EP system onboard. Therefore, the additional mass of the deorbit system, when using EP, is not only the mass of propellant, but also the mass of every hardware component of the EP system (such as mass of propellant tanks, mass of the thruster, mass of the power unit for the thruster, etc.). this inert mass will then be accounted as additional mass required for deorbit, when comparing different deorbit systems. Typical features of EP are much longer time of re-entry with respect to chemical propulsion, high I<sub>sp</sub>, but very low thrust levels (again with respect to chemical propulsion Ion and plasma thrusters are the best





performing solutions, but they should be avoided since they are generally too expensive to be used for deorbit. Hall thrusters are, instead, the best option among the family of EP systems. They represent the optimum compromise between minimizing cost and achieving sufficient performance.

The MATLAB code works by integrating with respect to time a second order differential equation using the ode45 solver, Figure 4. The equation uses as initial values the upper-stage state vector (1) and (2).

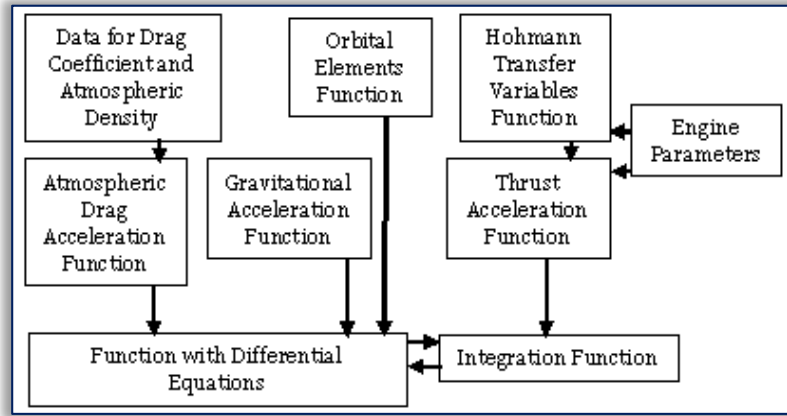


Figure 4. MATLAB Simulation Methodology Scheme

$$\dot{v}_{us} = g_{us} - \frac{v_{us}}{\|v_{us}\|} a_{drag} - \frac{v_{us}}{\|v_{us}\|} a_T \quad (1)$$

$$X_{us} = [r_{us} \ v_{us}] = [x_{us} \ y_{us} \ z_{us} \ v_{x_{us}} \ v_{y_{us}} \ v_{z_{us}}] \quad (2)$$

$$\dot{X}_{us} = [\dot{r}_{us} \ \dot{v}_{us}] = [\dot{x}_{us} \ \dot{y}_{us} \ \dot{z}_{us} \ \dot{v}_{x_{us}} \ \dot{v}_{y_{us}} \ \dot{v}_{z_{us}}] \quad (3)$$

Initially, engine specific parameters taken from Table 8 are used to calculate the Hohmann transfer variables,  $\Delta v$ ,  $\Delta t$ , and necessary fuel mass, (33-37). These results are then utilized when calculating the thrust acceleration,  $a_T$  in (1). The constants shown in Table 9 have been used in the calculation of the gravitational acceleration. Equations (4) - (15) are components of a function used to calculate the gravitational acceleration having the spacecraft position vector as input. The function outputs the gravitational acceleration in the x, y, z directions, for which (13), (14) and (15) are used, [8]. These outputs are used by the ode45 solver and integrated with respect to time.

Table 9. Constants used in the geopotential model

Mass of Earth	$M_E = 5.972 \cdot 10^{24} \text{ kg}$
Earth Equatorial Radius	$R_E = 6372.137 \text{ km}$
Gravitational Constant	$G = 6.673 \cdot 10^{-20} \frac{\text{km}^3}{\text{kg} \cdot \text{s}}$
J2 Parameter	$J_2 = 1.08263 \cdot 10^{-3}$
J3 Parameter	$J_3 = -2.5321 \cdot 10^{-6}$
J4 Parameter	$J_4 = -1.610987 \cdot 10^{-6}$

$$R_{mag} = \|r_{us}\| \quad (4)$$

$$R_{R2} = \left( \frac{R_E}{R_{mag}} \right)^2 \quad (5)$$

$$R_{R3} = \left( \frac{R_E}{R_{mag}} \right)^3 \quad (6)$$

$$R_{R4} = \left( \frac{R_E}{R_{mag}} \right)^4 \quad (7)$$

$$z_R = \frac{z_{us}}{R_{mag}} \quad (8)$$

$$z_{R2} = \left( \frac{z_{us}}{R_{mag}} \right)^2 \quad (9)$$

$$z_{R4} = \left( \frac{z_{us}}{R_{mag}} \right)^4 \quad (10)$$

$$q = 1 + 1.5 \cdot J_2 \cdot R_{R2} (1 - 5z_{R2}) + 2.5 \cdot J_3 \cdot R_{R3} (3 - 7z_{R2}) z_R - 4.375 \cdot J_4 \cdot R_{R4} \left( 9z_{R4} - 6z_{R2} + \frac{3}{7} \right) \quad (11)$$

$$\mu = G_E M_E \quad (12)$$

$$g_x = -\frac{\mu}{R_{mag}^3} x_{us} q \quad (13)$$

$$g_y = -\frac{\mu}{R_{mag}^3} y_{us} q \quad (14)$$





$$g_z = -\frac{\mu}{R_{\text{mag}}^2} \left\{ \left[ (1 + 1.5J_2 R_{R2} (3 - 5z_{R2})) z_R + (2.5J_3 R_{R3} (6z_{R2} - 7z_{R4} - 0.6)) \right. \right. \\ \left. \left. + \left( -4.375J_4 R_{R4} \left( \frac{15}{7} - 10z_{R2} + 9z_{R4} \right) z_R \right) \right] \right\} \quad (15)$$

(16) is used for the determination of the acceleration caused by the atmospheric drag force, in which CD is the drag coefficient and  $\rho$  is the atmospheric density, values for which are taken from [9] and [10].

$$a_{\text{Drag}} = -\frac{1}{2m} CDA\rho v_{\text{us}}^2 \frac{v_{\text{us}}}{v_{\text{us}}} \quad (16)$$

The following algorithm, equations (17-32), [11], defines the orbital elements, where  $r$  is the Earth – Moon distance,  $v$  is the Moon's orbital speed,  $v_r$  is the Moon's radial speed,  $h$  is the Moon's orbital angular momentum,  $N$  is the vector node line of the Moon's orbit,  $\Omega$  is the right ascension of the ascending node,  $e$  is the Moon's orbit eccentricity vector,  $\omega$  is the Moon's orbit argument of periapsis,  $\theta$  is the Moon's orbit true anomaly,  $a$  is the Moon's orbit semi-major axis,  $T$  is the Moon's orbital period and  $M$  is the Moon's orbit mean anomaly.

$$r = \sqrt{r \cdot r} \quad (17)$$

$$v = \sqrt{v \cdot v} \quad (18)$$

$$v_r = \frac{r \cdot v}{r} \quad (19)$$

$$h = r \times v = \begin{bmatrix} \hat{i} & \hat{j} & \hat{k} \\ X & Y & Z \\ v_x & v_y & v_z \end{bmatrix} \quad (20)$$

$$h = \sqrt{h \cdot h} \quad (21)$$

$$i = \text{Cos}^{-1} \left( \frac{h_z}{h} \right) \quad (22)$$

$$N = \hat{k} \times h = \begin{bmatrix} \hat{i} & \hat{j} & \hat{k} \\ 0 & 0 & 0 \\ h_x & h_y & h_z \end{bmatrix} \quad (23)$$

$$N = \sqrt{N \cdot N} \quad (24)$$

$$\Omega = \begin{cases} \text{Cos}^{-1} \left( \frac{N_x}{N} \right), & N_y \geq 0 \\ 360^\circ - \text{Cos}^{-1} \left( \frac{N_x}{N} \right), & N_y < 0 \end{cases} \quad (25)$$

$$e = \frac{1}{\mu} \left[ \left( v^2 - \frac{\mu}{r} \right) r - r v_r v \right] \quad (26)$$

$$e = \sqrt{e \cdot e} \quad (27)$$

$$\omega = \begin{cases} \text{Cos}^{-1} \left( \frac{N \cdot e}{Ne} \right), & e_z \geq 0 \\ 360^\circ - \text{Cos}^{-1} \left( \frac{N \cdot e}{Ne} \right), & e_z < 0 \end{cases} \quad (28)$$

$$\theta = \begin{cases} \text{Cos}^{-1} \left( \frac{e \cdot r}{er} \right), & v_r \geq 0 \\ 360^\circ - \text{Cos}^{-1} \left( \frac{e \cdot r}{er} \right), & v_r < 0 \end{cases} \quad (29)$$

$$a = \frac{h^2}{\mu} \frac{1}{1 - e^2} \quad (30)$$

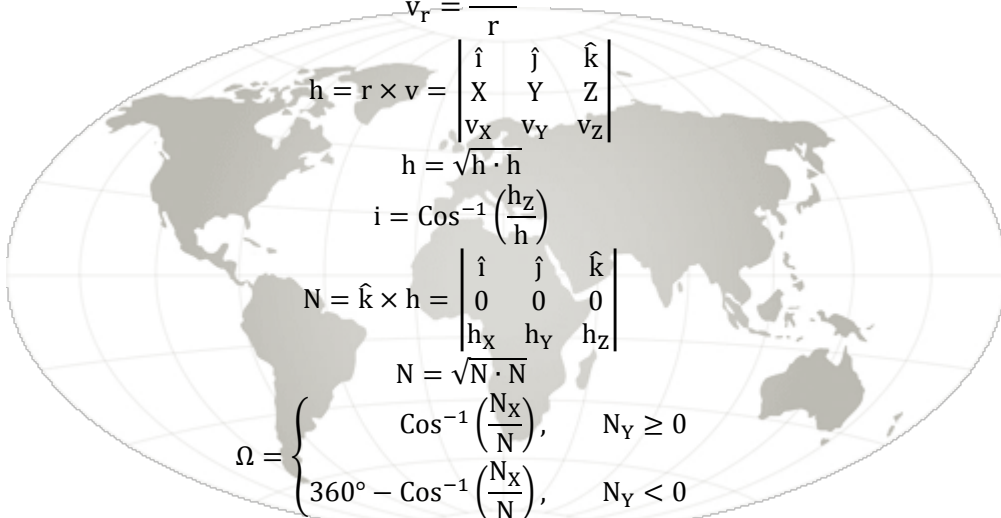
$$T = \frac{2\pi}{\sqrt{\mu}} a^{\frac{3}{2}} \quad (31)$$

$$M = \frac{2\pi}{T} \quad (32)$$

$$e = \frac{r_a - r_p}{r_a + r_p} \quad (33)$$

$$h = \sqrt{r_{p(a)} \mu (1 + e \cos \theta)} \quad (34)$$

$$v_{p(a)} = \frac{h}{r_{p(a)}} \quad (35)$$





$$m_f = m_0 \left( e^{\frac{\Delta v}{I_{sp} g_0}} - 1 \right) \quad (36)$$

$$\Delta t = m_0 \frac{\Delta v}{T} \quad (37)$$

#### 4. NUMERICAL SIMULATION RESULTS

As seen in Table 11, propulsion systems are very effective in deorbiting a 418 kg upper-stage from LEO at EOM, with the best results being obtained for a cluster of four 306 N thrust double base propellant SRMs. Although the necessary fuel mass to achieve  $\Delta v$  is unrealistic concerning the given engine/motor, the values hold true for the given thrust and specific impulse. The PPT is the worst deorbiting device, fulfilling deorbiting in 4 days, but it still complies by far with the '25 years' mitigation rule. Although every engine/motor must achieve the same  $\Delta v$ , the final deorbiting time is different because of the varying mass of each system.

Table 10. Numerical simulations results

Propulsion Category	Engine	Thrust [N]	Isp [s]	Mass [kg]	Nr. of used engines	$\Delta t$	$m_f$ [kg]	Deorbit time
Double base propellant	STAR 4G	306.927	269.4	1.49	4	2.26s	364	16 min.
Bipropellant	R-4D	445	312	3.76	2	1.59s	307	16 min
Monopropellant	MR-107	275	236	0.88	3	3.34s	661	19 min.
Cold gas propellant	Sterer	12	68	0.174	6	38s	1740	25 min.
Resistojet	MR-501B	0.3	300	0.89	4	39min	314	31 min.
Arcjet	Primex MR-510	0.235	580	1.58	4	49min	141	31 min.
Ion contact thruster	XIPS	0.015	2800	6.5	2	26h	54	4h
Hall Effect Thruster	Fakel SPT-70	0.04	1510	1	2	9h	104	1h
PPT	Les 8/9	0.0003	600	5	2	27days	140	4 days

For a detailed description of the perturbation of thrust on the orbital trajectory, in Figures 5 – 16, are represented the variation in perturbation and orbital elements for the XIPS ion contact thruster. Figure 5 presents the variation in altitude for deorbiting a 418 kg upper-stage from 2011 km with the XIPS ion contact thruster. Figure 6 presents the variation in atmospheric drag acceleration for deorbiting a 418 kg upper-stage from 2011 km with the XIPS ion contact thruster.

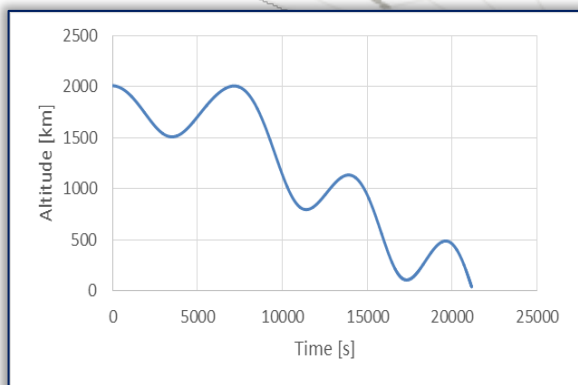


Figure 5. Altitude variation in the case of deorbiting with the XIPS Ion Contact Thruster from an initial altitude of 2011 km

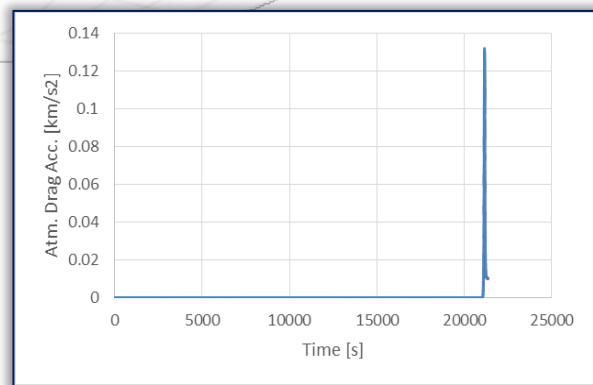


Figure 6. Atmospheric Drag Acceleration variation in the case of deorbiting with the XIPS Ion Contact Thruster from an initial altitude of 2011 km

Figure 7 presents the variation in thrust acceleration or deorbiting a 418 kg upper-stage from 2011 km with the XIPS ion contact thruster. Figure 8 presents the variation in inclination for deorbiting a 418 kg upper-stage from 2011 km with the XIPS ion contact thruster.

Figure 9 presents the variation in argument of periapsis or deorbiting a 418 kg upper-stage from 2011 km with the XIPS ion contact thruster. Figure 10 presents the variation in RAAN for deorbiting a 418 kg upper-stage from 2011 km with the XIPS ion contact thruster.

Figure 11 presents the variation in true anomaly or deorbiting a 418 kg upper-stage from 2011 km with the XIPS ion contact thruster. Figure 12 presents the variation in eccentricity for deorbiting a 418 kg upper-stage from 2011 km with the XIPS ion contact thruster.



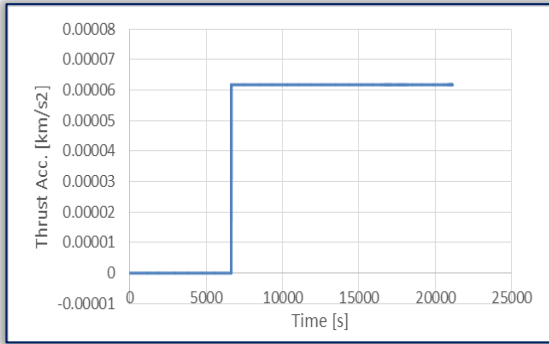


Figure 7. Thrust Acceleration variation in the case of deorbiting with the XIPS Ion Contact Thruster from an initial altitude of 2011 km

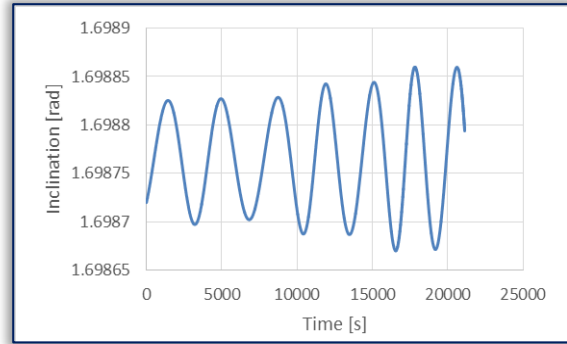


Figure 8. Inclination variation in the case of deorbiting with the XIPS Ion Contact Thruster from an initial altitude of 2011 km

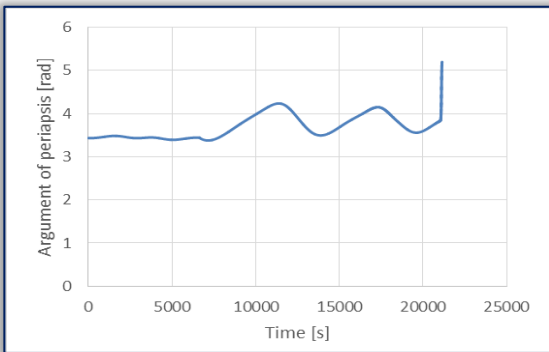


Figure 9. Argument of Periapsis variation in the case of deorbiting with the XIPS Ion Contact Thruster from an initial altitude of 2011 km

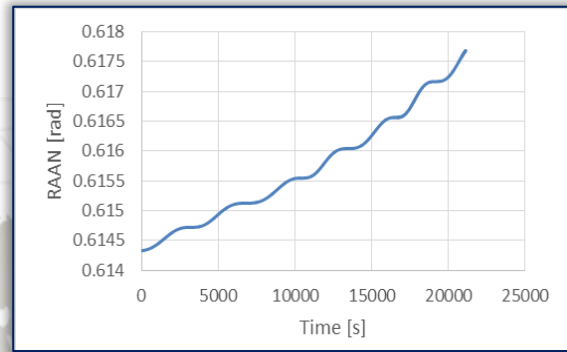


Figure 10. RAAN variation in the case of deorbiting with the XIPS Ion Contact Thruster from an initial altitude of 2011 km

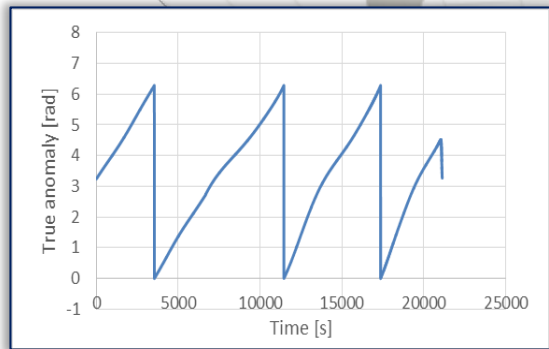


Figure 11. True Anomaly variation in the case of deorbiting with the XIPS Ion Contact Thruster from an initial altitude of 2011 km

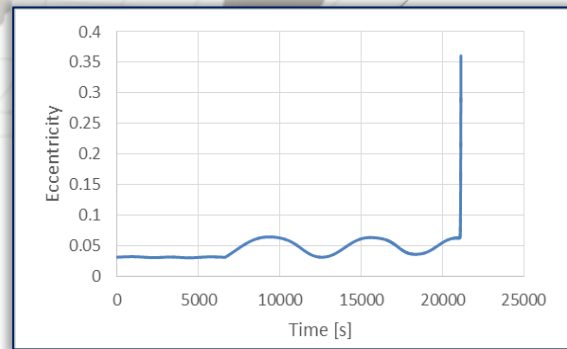


Figure 12. Eccentricity variation in the case of deorbiting with the XIPS Ion Contact Thruster from an initial altitude of 2011 km

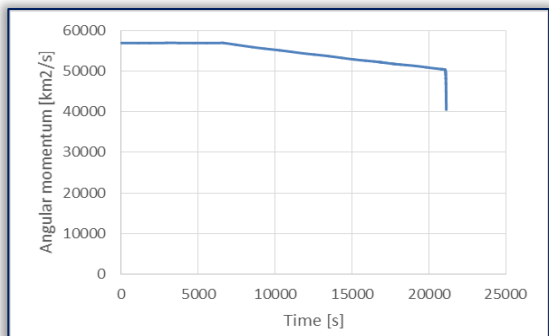


Figure 13. Orbital Angular Momentum variation in the case of deorbiting with the XIPS Ion Contact Thruster from an initial altitude of 2011 km

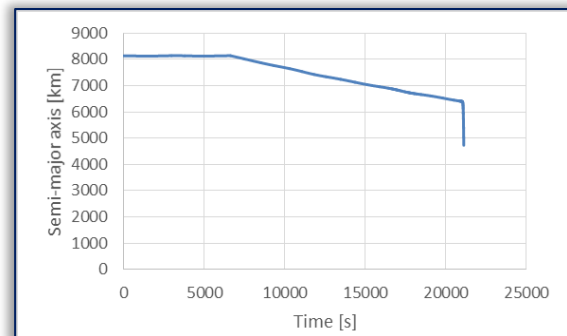


Figure 14. Semi-major Axis variation in the case of deorbiting with the XIPS Ion Contact Thruster from an initial altitude of 2011 km





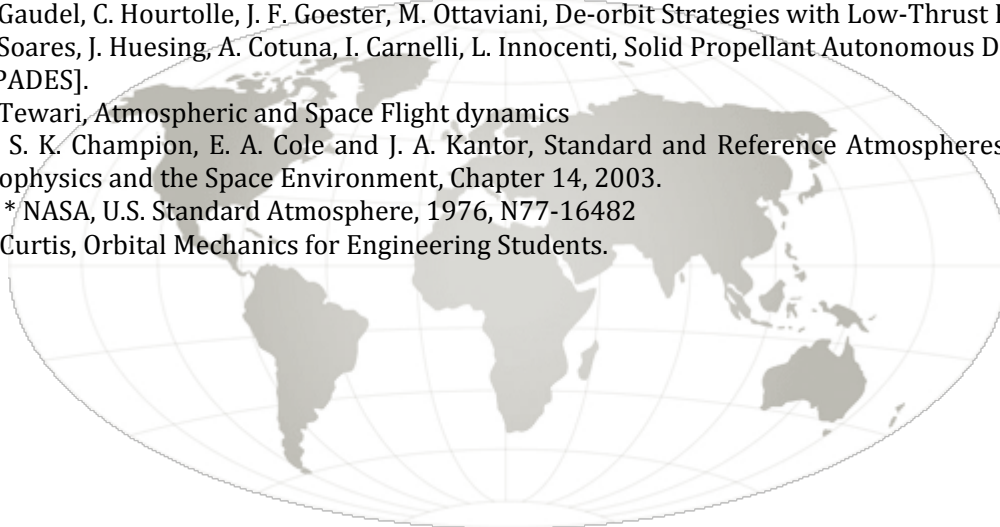
Figure 13 presents the variation in orbital angular momentum or deorbiting a 418 kg upper-stage from 2011 km with the XIPS ion contact thruster. Figure 14 presents the variation in eccentricity for deorbiting a 418 kg upper-stage from 2011 km with the XIPS ion contact thruster.

## CONCLUSIONS

The performance study made in this research paper concludes the efficiency of using chemical and electrical propulsion when deorbiting a 418 kg upper-stage from LEO at its end-of-mission. The deorbiting devices by far respect the '25 years' deorbiting mitigation rule. Future work includes specific propulsion system performance assessment as well as considering different deorbiting scenarios and strategies.

## References

- [1.] A. Jenkin, M. Sorge, G. Peterson, J. McVey, B. Yoo, Predicting the Future Space Debris Environment, Crosslink, Vol. 16, No. 1, 2015.
- [2.] M. Sorge, G. Peterson, How to Clean Space: Disposal and Active Debris Removal, Crosslink, Vol. 16, No. 1, 2015.
- [3.] R. Janovsky, M. Kassebom, H. Lubberstedt, O. Romberg, H. Burkhardt, M. Sippel, G. Krulle, B. Fritsche, End-of-Life De-Orbiting Strategies for Satellites, IAA 03-5.4.05.
- [4.] G. Pastore, Debris Mitigation in LEO Orbits: Performance Analysis and Comparison of different Deorbit Systems.
- [5.] R. A. C. Schonenberg, H. F. R. Schoyer, Solid Propulsion De-orbiting and Re-orbiting.
- [6.] A. Gaudel, C. Hourtolle, J. F. Goester, M. Ottaviani, De-orbit Strategies with Low-Thrust Propulsion.
- [7.] T. Soares, J. Huesing, A. Cotuna, I. Carnelli, L. Innocenti, Solid Propellant Autonomous De-Orbit System [SPADES].
- [8.] A. Tewari, Atmospheric and Space Flight dynamics
- [9.] W. S. K. Champion, E. A. Cole and J. A. Kantor, Standard and Reference Atmospheres, Handbook of Geophysics and the Space Environment, Chapter 14, 2003.
- [10.] \*\*\* NASA, U.S. Standard Atmosphere, 1976, N77-16482
- [11.] H. Curtis, Orbital Mechanics for Engineering Students.



ANNALS of Faculty Engineering Hunedoara  
- International Journal of Engineering



copyright © UNIVERSITY POLITEHNICA TIMISOARA,  
FACULTY OF ENGINEERING HUNEDOARA,  
5, REVOLUTIEI, 331128, HUNEDOARA, ROMANIA  
<http://annals.fih.upt.ro>

